THE JOURNAL OF BIOLOGICAL CHEMISTRY VOL. 284, NO. 29, pp. 19744–19753, July 17, 2009

Intestinal Anion Exchanger Down-regulated in Adenoma (DRA) Is Inhibited by Intracellular Calcium*

Received for publication, April 4, 2009, and in revised form, May 14, 2009 Published, JBC Papers in Press, May 15, 2009, DOI 10.1074/jbc.M109.004127

Georg Lamprecht[‡1], Chih-Jen Hsieh[‡], Simone Lissner[‡], Lilia Nold[‡], Andreas Heil[‡], Veronika Gaco[‡], Julia Schäfer[‡], Jerrold R. Turner[§], and Michael Gregor[‡]

From the [‡]1st Medical Department, University of Tübingen, 72076 Tübingen, Germany and the [§]Department of Pathology, University of Chicago, Chicago, Illinois 60637

The Na/H exchanger 3 (NHE3) and the Cl/HCO_3 exchanger down-regulated in adenoma (DRA) together facilitate intestinal electroneutral NaCl absorption. Elevated Ca^{2+}_i inhibits NHE3 through mechanisms involving the PDZ domain proteins NHE3 kinase A regulatory protein (E3KARP) or PDZ kidney 1 (PDZK1). DRA also possesses a PDZ-binding motif, but the roles of interactions with E3KARP or PDZK1 and Ca^{2+}_i in DRA regulation are unknown. Wild type DRA and a mutant lacking the PDZ interaction motif (DRA-ETKFminus) were expressed constitutively in human embryonic kidney (HEK) and inducibly in Caco-2/BBE cells. DRA-mediated Cl/HCO_3 exchange was measured as intracellular pH changes. Ca^{2+}_i was assessed fluorometrically. DRA was induced 8–16-fold and was delivered to the apical surface of polarized Caco-2 cells. Putative anion transporter 1 and cystic fibrosis transmembrane regulator did not contribute to Cl/HCO_3 exchange in transfected Caco-2 cells. The calcium ionophore 4Br-A23187 inhibited DRA and DRA-ETKFminus in HEK cells, but only full-length DRA was inhibited in Caco-2 cells. In contrast, 100 μM UTP, which increased Ca^{2+}_i, inhibited full-length DRA but not DRA-ETKFminus in Caco-2 and HEK cells. In HEK cells, which express little PDZK1, additional transfection of PDZK1 was required for UTP to inhibit DRA. As HEK cells do not express cystic fibrosis transmembrane regulator or NHE3, the data indicate that Ca^{2+}_i-dependent DRA inhibition is not because of modulation of other transport activities. In polarized epithelium, this inhibition requires interaction of DRA with PDZK1. Together with data from PDZK1$^{-/-}$ mice, these data underscore the prominent role of PDZK1 in Ca^{2+}_i-mediated inhibition of colonic NaCl absorption.

In the gastrointestinal tract electroneutral NaCl absorption occurs in the distal ileum and proximal colon by parallel Na/H exchange and Cl/HCO_3 exchange. Studies in knock-out mice have confirmed that NHE3[2] (Na/H exchanger, isoform 3; SLC9A3) and DRA (down-regulated in adenoma; SLC26A3) are the primary transporters responsible for these events (1, 2). The importance of the latter is emphasized by the human genetic disorder congenital chloride diarrhea (3), in which a nonfunctional DRA leads to life-threatening diarrhea. DRA is also expressed in the duodenum (in the lower villus) and in the pancreas (4–6), where it is involved in chloride and bicarbonate secretion together with CFTR (4–7). All three transport proteins, NHE3, DRA, and CFTR, have PDZ interaction motifs that facilitate binding to several members of the NHERF class of PDZ adapter proteins (8, 9).

Electroneutral NaCl absorption is regulated largely in parallel but reciprocally with electrogenic chloride secretion (10). In different systems NHE3 is acutely regulated by cAMP, cGMP, intracellular calcium, lysophosphatidic acid, and epidermal growth factor (11) as well as by tumor necrosis factor-α (12). Notably, some of these regulatory processes are mediated through the interaction of NHE3 with several members of the NHERF class of PDZ adapter proteins (8, 11).

Relatively little is known about the acute regulation of DRA. In the context of chloride and bicarbonate secretion, DRA is activated by cAMP, if it is expressed in a complex with CFTR and PDZ adapter proteins (PDZK1, also known as CAP70, and/or NHERF) (6, 7, 13). It is expected that DRA is inhibited *in vivo* in parallel with NHE3 during NaCl absorption, and in Caco-2/BBE cells transfected with NHE3 and DRA, this coupled inhibition has recently been shown (14). In *Xenopus* oocytes DRA is refractory to regulation by the calmodulin antagonist calmidazolium (10 μM), the PP2A inhibitor calyculin A (100 nM), or actin-modifying agents (13). Other data suggest that direct phosphorylation may regulate DRA, as mutation of tyrosine 756 (Y756F) increases DRA activity, although no signaling pathway has been suggested (13). Thus the regulation of DRA remains poorly understood. Moreover, no data address whether DRA regulation can occur independently or is always dependent on regulation of partner transporters, *i.e.* CFTR or NHE3, to which it is functionally and structurally coupled.

Here we show that DRA activity is inhibited by elevations of Ca^{2+}_i, that this regulation is independent of CFTR and NHE3, and that regulation requires interactions between DRA and the PDZ adapter protein PDZK1.

* This work was supported by Deutsche Forschungsgemeinschaft Grants La 1066/3-2 and La 1066/3-3.

[1] To whom correspondence should be addressed. Tel.: 49-7071-2987108; Fax: 49-7071-295221; E-mail: hans-georg.lamprecht@uni-tuebingen.de.

[2] The abbreviations used are: NHE3, Na/H exchanger isoform 3; CFTR, cystic fibrosis transmembrane regulator; DRA, down-regulated in adenoma (SLC26A3); PAT1, putative anion transporter 1 (SLC26A6); NHERF, NHE3 regulatory factor; E3KARP, NHE3 kinase A regulatory protein; PDZK1, PDZ domain protein kidney 1; IKEPP, intestinal and kidney enriched PDZ protein; PKC, protein kinase C; PMA, phorbol myristate acetate; EGFP, enhanced green fluorescent protein; RT, reverse transcription; PBS, phosphate-buffered saline; HEK, human embryonic kidney; pH_i, intracellular pH; DIDS, 4,4′-diisothiocyanostilbene-2,2′-disulfonic acid.

EXPERIMENTAL PROCEDURES

Materials—Trypsin, doxycycline, hygromycin, G418, and Zeocin were from Invitrogen. 4Br-A23187 and PMA were from Biomol. Sulfo-NHS-SS-biotin and NeutrAvidin were from Pierce. Alexa594-conjugated phalloidin, 2′,7′-bis(carboxyethyl)-5,6-carboxyfluorescein-acetoxymethyl ester, and FURA-2-AM were from Molecular Probes. Nigericin and all other chemicals were from Sigma.

Cell Culture and Transfection—In our previous study we have used a mixed population of HEK cells stably transfected with EGFP-tagged wild type DRA (15). A full-length EGFP-tagged DRA construct lacking the PDZ interaction domain (*i.e.* lacking the C-terminal four amino acids ETKF) was cloned into pEGFP-C1 (Clontech). HEK cells were transfected with pEGFP/DRA (wild type) and pEGFP/DRA-ETKFminus, as described previously (15), and clonal cell lines were established by serial dilution. Two randomly chosen clones with comparable Cl/HCO_3 exchange activity were used for further studies.

EGFP-DRA and EGFP-DRA-ETKFminus fusion constructs were subcloned into pTRE2[hygro]. Caco-2/BBE cells stably transfected with the Tet-Off system (16) were transfected in suspension while passaging the cells and grown for 24 h in the absence of antibiotics. Cells were then passaged again and diluted onto 100-mm dishes. The parental cell line is already G418- and Zeocin-resistant, and transfected cells were thus selected using 250 μg/ml G418, 50 μl/ml Zeocin, and 200 μg/ml hygromycin in Dulbecco's modified Eagle's medium plus 10% fetal calf serum and 0.5% penicillin/streptomycin. Clones appeared after 14–21 days, and those that showed green fluorescence were recovered using cloning rings (Sigma). Two randomly chosen clones with comparable Cl/HCO_3 exchange activity were used for further studies. Cells were used between passages 5 and 12 after transfection. They were grown and split in the presence of 20 ng/ml doxycycline, and only cells used for functional studies were kept in the absence of doxycycline immediately after passaging the cells.

PDZK1 was cloned by RT-PCR from a human ileal biopsy (sense primer, CTC TTG GAT CCC CAG AAA TGA CCT CCA CC, and antisense primer, AAG CTT TTA CTT GTT TTC ATC ACA TCT CTG). The sequence was verified in pCR-II-blunt, and the insert was subcloned into pEGFP resulting in pEGFP/PDZK1. HEK/EGFP-DRA cells were transfected with EGFP-PDZK1 as described previously (15), and clonal cell lines were established by serial dilution.

Confocal Microscopy—Cells were washed with PBS, fixed for 10 min in 3.7% formaldehyde in PBS, and washed again in PBS. They were then permeabilized for 5 min using 1% Triton X-100 in PBS, washed, and blocked for 20 min using 1% bovine serum albumin in PBS. The actin cytoskeleton was stained using Alexa594/phalloidin (1:200 in PBS). The samples were washed again three times in PBS and mounted using SlowFade (Molecular Probes). The slides were visualized using a confocal microscope (LSM510, Zeiss).

Measurement of Intracellular pH and Intracellular Calcium—DRA activity was assessed as changes in the intracellular pH (pH_i) after removing chloride from the extracellular buffer. In transfected HEK cells, pH_i was measured exactly as described previously (15). In transfected Caco-2/BBE cells, pH_i was measured as described previously (15) with minor modifications. Because of the slow calibration of confluent Caco-2/BBE cells, a one-point calibration at pH 7.0 was performed in some experiments as described by Boyarsky *et al.* (17) after validating this approach using the conventional calibration at pH 7.0, 7.5, and 7.8. The base-line pH_i of the transfected Caco-2/BBE cells varied from day to day. To analyze experiments from several days, data for these cells are expressed as ΔpH_i compared with base line.

The pH_i traces from the transfected HEK cells were analyzed as described previously (18). This nonlinear curve-fitting algorithm allows the estimation of the initial slope after the change of the buffer solutions as well as the estimation of the maximal pH_i change from base line after removal of extracellular chloride. For the transfected Caco-2/BBE cells, ΔpH_i values were used in this algorithm instead of absolute pH_i values.

For calcium measurements, cells were loaded with 1 μM FURA-2-AM for 60 min. The sample was excited alternating at 340 and 380 nm (slit width 2.5 nm), and emission was collected at 510 nm (slit width 2.5–3.5 nm). Data were recorded every 2.9 s. Intracellular calcium concentration was expressed as the F_{380}/F_{340} ratio.

Semiquantitative RT-PCR—RNA was prepared using the RNAqueous kit (Ambion) according to the recommendations of the manufacturer from 10-day confluent Caco-2/BBE cells, in which expression of EGFP-DRA or EGFP-DRA-ETKFminus was either repressed by the presence of doxycycline or induced by its absence. cDNA was synthesized using Superscript reverse transcriptase (Invitrogen). PCR was carried out with 50 ng of cDNA template in an ABI Prism 7000 system using the SYBR green method. DRA (endogenous DRA and induced EGFP-DRA), EGFP (induced EGFP-DRA), PAT1, CFTR, NHE3, PDZK1, and E3KARP as well as histone 3.3A were amplified using the following primers that were optimized for amplification efficiency: histone 3.3A, TTCCAGAGCGCAGCTATCG (300 nM) and TCTTCAAAAAGGCCAACCAGAT (300 nM); DRA, GTGTCCTTTCTTGATGTTTCTTCAGT (200 nM) and CGGTTAAGCTTCTCAATGAAGTCA (200 nM); EGFP, CAAGCAGAAGAACGGCATCAC (300 nM) and GGACTGGGTGCTCAGGTAGGC (300 nM); PAT1, GGGTGCCCTCTCCTTTGTG (300 nM) and CCAGATGGGTCCACACTGAAG (300 nM); CFTR, GGAAAAGGCCAGCGTTGTC (250 nM) and CCAGGCGCTGTCTGTATCCT (250 nM); NHE3, CTGTCCCTCTACGGCGTCTT (100 nM) and GCTGCCAAACAGGAGGAAGTC (300 nM), PDZK1, TGGAGGTGTGCAAACTTGGA (200 nM) and ACACCCCCTTTTTACCTTGGA (200 nM); and E3KARP, GTCACCCGTCACCAATGGA (300 nM) and CAGTGTCCTTGTCGGAACCA (200 nM). The data were analyzed by the $\Delta\Delta C_t$ method ($\Delta\Delta C_t = (C_t^{\text{sample}} - C_t^{\text{reference}})^{\text{doxycycline}} - (C_t^{\text{sample}} - C_t^{\text{reference}})^{\text{no-doxycycline}}$).

Surface Expression of EGFP-DRA in Transfected Caco-2/BBE Cells—Cell surface expression was assayed by biotinylation similar to that described in Ref. 19. 10-Day confluent Caco-2/BBE cells expressing EGFP-DRA were washed three times with PBS (plus calcium and magnesium). The cells were then incubated twice for 30 min with 1 mg/ml sulfo-NHS-SS-biotin

(Pierce) in PBS (plus calcium and magnesium). After removal of the buffer, unbound biotin was quenched with 5 mg/ml iodoacetamide in PBS (plus calcium and magnesium) plus 1% bovine serum albumin for 5 min. The cells were then scraped and lysed in 1 ml of 60 mM HEPES, 154 mM NaCl, 3 mM KCl, 5 mM NaEDTA, 3 mM NaEGTA, 1% Triton X-100, and 125 μl/ml complete protease inhibitor mixture (Roche Applied Science) by passing them 15 times through a 22-gauge needle. The lysates were cleared by spinning for 10 min at 10,000 $\times$ *g* and were then incubated with 100 μl of NeutrAvidin-agarose beads overnight. Beads were separated by centrifugation for 1 min at 2500 $\times$ *g*, and bound proteins were eluted by boiling in 2$\times$ Laemmli sample buffer for 3 min. 30 μl of the lysate and 60 μl of the eluate from the beads were separated on 8.5% SDS-PAGE, blotted onto nitrocellulose (Schleicher & Schüll), and probed with monoclonal anti-EGFP antibody (1:500; Clontech) and anti-mouse (1:5000) secondary antibody (Jackson ImmunoResearch) using standard conditions. Bands were quantified using ImageMaster 1D, version 3.0 software (Amersham Biosciences), with manual background subtraction. Relative changes of DRA surface expression were analyzed by normalization of the band intensity of biotinylated EGFP-DRA to the band intensity of total EGFP-DRA in the lysate.

Immunoblotting of PDZ Adapter Proteins—NHERF and E3KARP were detected using antibodies described previously (20, 21) at a dilution of 1:3000 each. PDZK1 and IKEPP were detected using commercially available antibodies (catalogue numbers PA3-16818 and PA3-16819ABR, Golden, CO) at a dilution of 1:1000 each. Anti-rabbit secondary antibody (Jackson ImmunoResearch) was used 1:5000.

Statistical Analysis—All statistical calculations were done using Jump 5.1 (SAS Institute, Cary, NC). All data are presented as means $\pm$ S.D. analysis of variance and *t* tests were applied when appropriate.

RESULTS

In HEK Cells Increased Intracellular Calcium Inhibits DRA Independently of Its PDZ Interaction Motif—Calcium-dependent short term regulation of NHE3 has been studied in transfected PS120 cells (19, 22). Thus we followed this approach and used our previously established HEK cells stably expressing EGFP-DRA (15). In these cells Cl/HCO_3 exchange is about eight times higher than in nontransfected cells. DRA activity was measured as intracellular alkalinization upon removal of chloride and intracellular re-acidification upon re-addition of chloride. Intracellular calcium was increased by 10 μM 4Br-A23187, which was applied 100 s before measuring DRA activity. Fig. 1*A* shows that 4Br-A23187 inhibited DRA activity both by a reduced pH_i change after removal of chloride (ΔpH_i, 0.58 $\pm$ 0.09 *versus* 0.36 $\pm$ 0.09, -39%, $p < 0.05$) as well as by a reduced initial slope (0.73 $\pm$ 0.22 pH/min *versus* 0.40 $\pm$ 0.17, -45%, $p < 0.05$). The limited background Cl/HCO_3 exchange in untransfected cells was not inhibited by 4Br-A23187, indicating that the effect is specific for DRA (data not shown). Taken together these data demonstrate that DRA is inhibited by intracellular calcium.

To address a role of PDZ adapter proteins in mediating the calcium effect, the experiment was repeated in two clonal cell

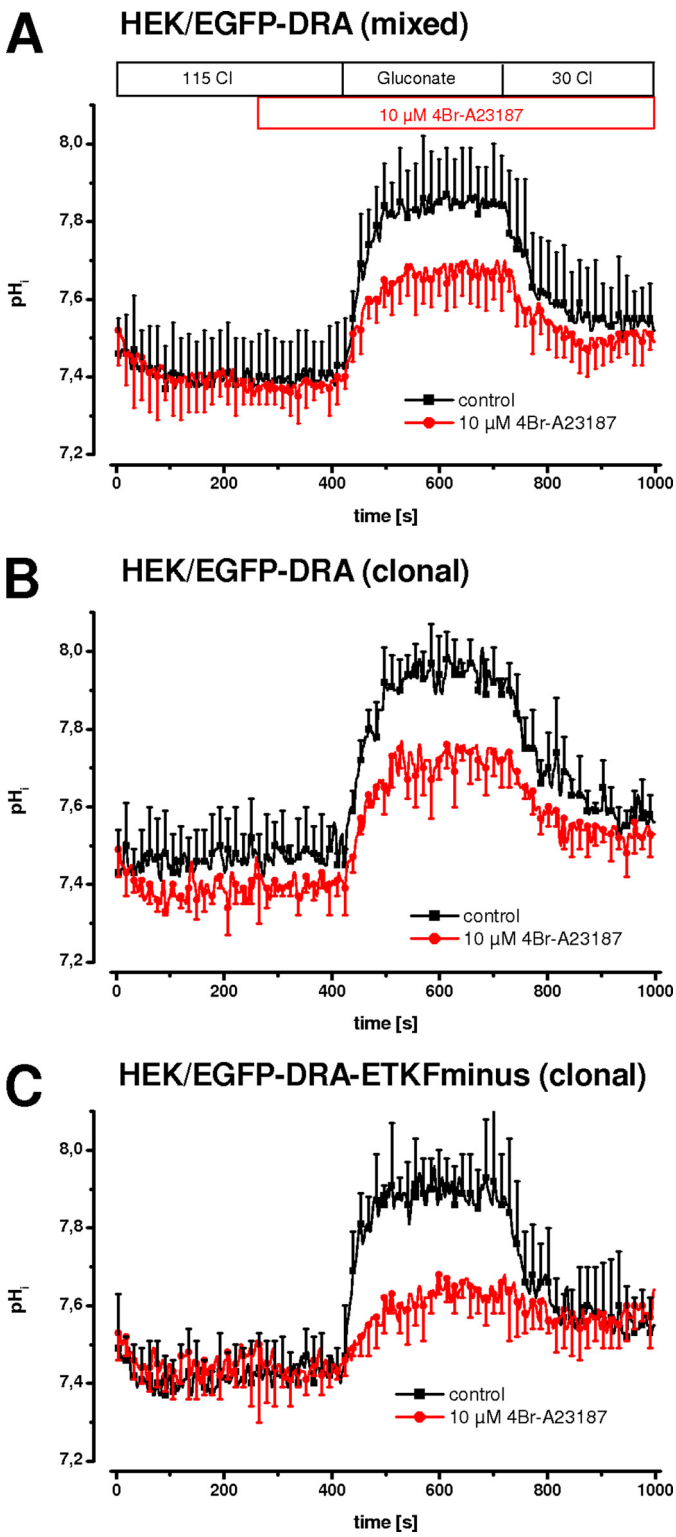

FIGURE 1. **In HEK cells 4Br-A23187 inhibits DRA independently of its PDZ interaction motif.** DRA activity was measured as intracellular alkalinization and reacidification upon chloride removal and readdition. Intracellular calcium was increased using 10 μM 4Br-A23187. *A,* in a mixed population (*i.e.* nonclonal) of HEK/EGFP-DRA cells, the maximal pH_i change and the initial slope are reduced by 39 and 45%, respectively (both $p < 0.05$) ($n = 8$–9 for each group). *B,* in HEK/EGFP-DRA clone 4 cells, the maximal pH_i change and the initial slope are reduced 28 and 33% (both $p < 0.05$) ($n = 4$–5 for each group). *C,* in HEK/EGFP-DRA-ETKF-minus clone 3 cells, the maximal pH_i change and the initial slope are reduced 49 and 80% (both $p < 0.05$) ($n = 4$–6 for each group).

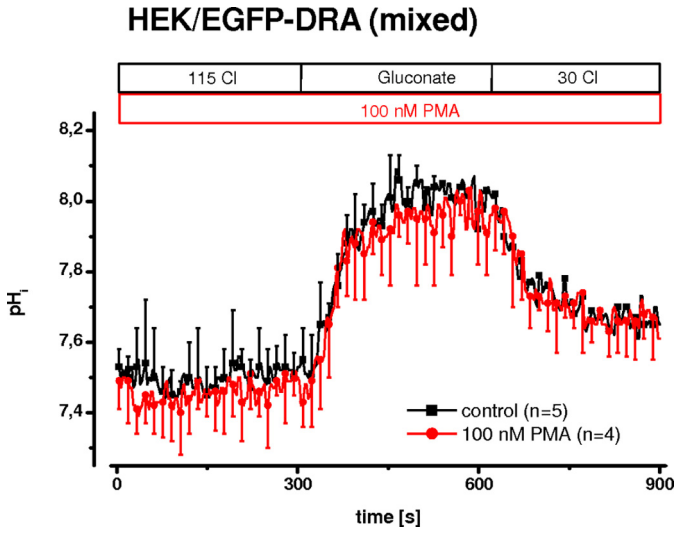

FIGURE 2. **PKC is not involved in calcium-mediated inhibition of DRA.** In a mixed population (*i.e.* nonclonal) of HEK/EGFP-DRA cells, PKC was activated using 100 nM PMA for 5 min ($n = 4–5$ for each group).

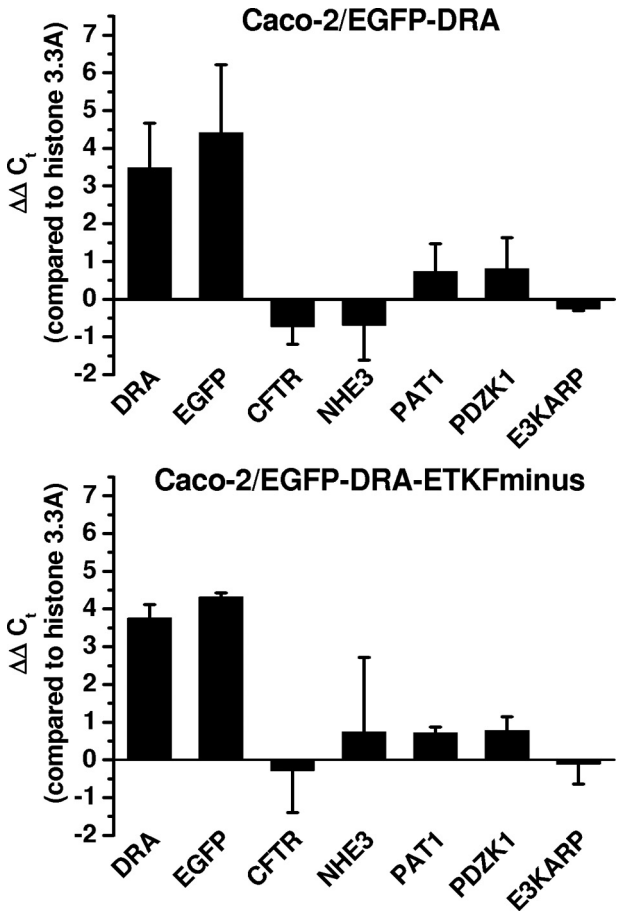

FIGURE 3. **Induction of EGFP-DRA by removal of doxycycline.** Relative changes of mRNA expression after removal of doxycycline were assessed by semiquantitative RT-PCR and normalization to the expression of histone 3.3A using the $\Delta\Delta C_t$ method. DRA and EGFP mRNA were induced to a similar extent by a factor of 8–16-fold (2^3 to 2^4). There was no significant induction or repression of mRNA expression of CFTR, PAT1, NHE3, PDZK1, or E3KARP in either EGFP-DRA- or EGFP-DRA-ETKFminus-expressing cells. Of note NHE3 was very poorly amplified by several primer pairs, explaining the large standard deviation. $n = 3$.

lines, one expressing wild type EGFP-DRA and one lacking the PDZ interaction motif (EGFP-DRA-ETKFminus) (Fig. 1, *B* and *C*). In EGFP-DRA (wild type) expressing HEK cells, the maximal pH$_i$ change after removal of chloride was reduced by 28% (ΔpH_i, 0.58 ± 0.08 *versus* 0.42 ± 0.07, $p < 0.05$), and the initial slope was reduced by 33% (0.60 ± 0.14 pH/min *versus* 0.40 ± 0.13, $p < 0.05$). In EGFP-DRA-ETKFminus-expressing HEK cells, the respective values were −49% (ΔpH_i, 0.60 ± 0.07 *versus* 0.30 ± 0.15, $p < 0.05$) and −80% (0.94 ± 0.16 pH/min *versus* 0.19 ± 0.11, $p < 0.05$). Thus calcium-mediated DRA inhibition induced by 4Br-A23187 was independent of the PDZ interaction motif arguing against a role of PDZ adapter proteins in transfected HEK cells.

Calcium-mediated Inhibition of DRA Does Not Involve Protein Kinase C—Cholinergic stimulation elicits a calcium signal that activates protein kinase C (PKC) by translocation to the apical plasma membrane and thus inhibits brush border NHE3 in the ileum (23). Furthermore, stimulation of PKC by phorbol ester has been shown to inhibit NHE3 in PS120 cells (24) and in Caco-2 cells (25). Given the parallel action of NHE3 and DRA, it appeared possible that the inhibition of DRA by calcium involved the activation of PKC. To test such an involvement, PKC was activated by 100 nM PMA for 5 min. Fig. 2 shows that DRA activity was unchanged after activation of PKC.

Stable Expression of DRA in Caco-2/BBE Cells—Because DRA regulatory pathways may not be present in poorly differentiated HEK cells, we expressed DRA and the ETKFminus mutant in the differentiated intestinal epithelial Caco-2/BBE cell line, which is a standard model of absorptive enterocytes. Our previous attempts to transgenically express DRA in Caco-2 cells have failed, perhaps because DRA expression retards growth in several transfected cell lines, with the notable exception of HEK cells (26). To circumvent this problem, Caco-2/BBE cells expressing the Tet-Off system (16) were transfected with EGFP-DRA and EGFP-DRA-ETKFminus in the Tet-responsive pTRE2[hygro] vector, and stable clones were selected by hygromycin in the presence of 20 ng/ml doxycycline, which suppresses the expression of the gene of interest. Clones were then tested for the expression of EGFP-DRA in the absence of doxycycline. Established clones were kept in culture in the continued presence of doxycycline except for those cells that were used for functional studies.

The effect of removal of doxycycline on the mRNA expression of EGF-DRA or EGFP-DRA-ETKFminus, PAT1 (SLC26A6), CFTR, and NHE3 as well as PDZK1 and E3KARP was assessed by semiquantitative RT-PCR (Fig. 3). Removal of doxycycline induced mRNA expression of DRA and DRA-ETKFminus as well as EGFP by a factor of 8–16-fold (2^3 to 2^4). Induction of EGFP was minimally (and statistically not significant) greater than induction of DRA indicating relatively little endogenous DRA expression compared with the induced expression of EGFP-DRA. mRNA expressions of PAT1, CFTR, NHE3, PDZK1, and E3KARP were all not significantly influenced by the induction of EGFP-DRA or EGFP-DRA-ETKFminus, and there were no differences between EGFP-DRA- and EGFP-DRA-ETKFminus-expressing cells. Of note, mRNA of NHE3 was difficult to amplify even with several other

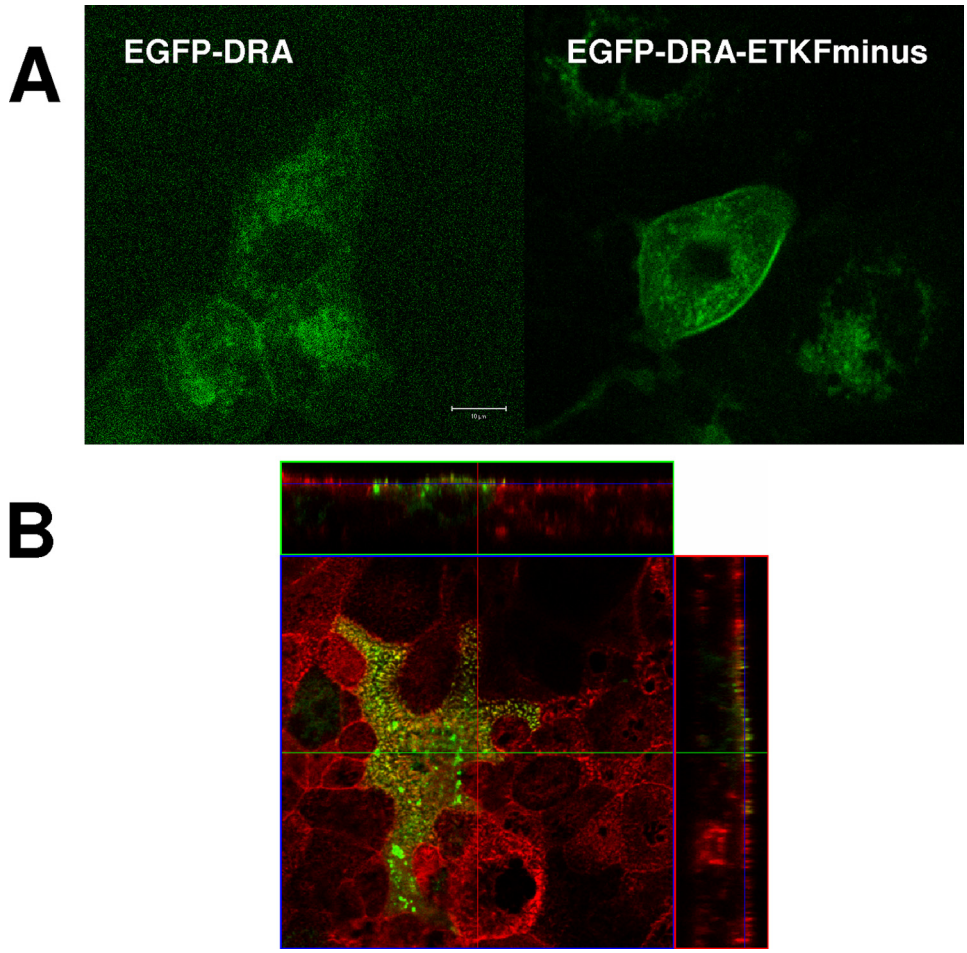

FIGURE 4. **DRA is expressed apically in transfected Caco-2/BBE cells.** *A,* EGFP-DRA and EGFP-DRA-ETKFminus autofluorescence in transfected Caco-2/BBE cells appears in a punctate manner suggesting expression in microvilli. *B,* this is supported by colocalization with the apical cytoskeleton, which was stained using Alexa594-labeled phalloidin.

primer pairs (C_t values >33) suggesting little endogenous NHE3 expression in these cells.

Expression of EGFP-DRA and EGFP-DRA-ETKFminus was confirmed by fluorescence microscopy for EGFP (Fig. 4*A*). EGFP-DRA and EGFP-DRA-ETKFminus are distributed at the apical surface in a punctate manner, suggestive of localization on microvilli. To further substantiate this, the actin cytoskeleton was counterstained. Fig. 4*B* shows that EGFP-DRA colocalizes with actin cores of apical microvilli. Similar images were obtained with EGFP-DRA-ETKFminus.

Possible Contribution of PAT1 and CFTR—mRNA of both PAT1 (SLC26A6) and CFTR was detected by RT-PCR in our cells (Fig. 3). PAT1 catalyzes Cl/HCO_3 exchange, and CFTR enhances PAT1 and DRA activity in several models (6, 7). Therefore, it was necessary to examine the influence of PAT1 and CFTR on the Cl/HCO_3 exchange activity in the EGFP-DRA-expressing Caco-2/BBE cells, *i.e.* after induction by doxycycline removal. Fig. 5 shows that Cl/HCO_3 exchange was not affected by 100

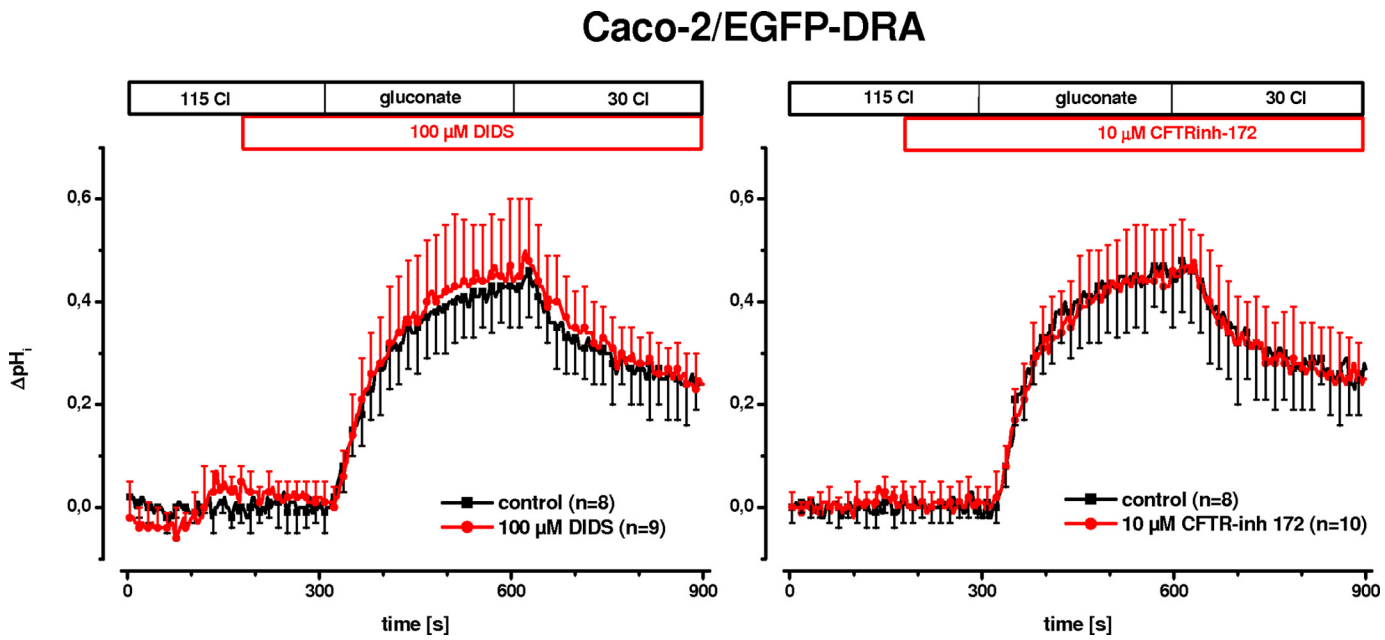

FIGURE 5. **PAT1 and CFTR do not contribute to Cl/HCO_3 exchange in Caco-2/BBE cells transfected with EGFP-DRA.** To address the potential contribution of PAT1 (SLC26A6) or CFTR in Cl/HCO_3 exchange of EGFP-DRA-transfected Caco-2/BBE cells, 100 μM DIDS (*left panel*) or 10 μM CFTRinh-172 (*right panel*) were applied before and during chloride removal and readdition. In both cases there was no statistical significant difference to control conditions, *i.e.* no inhibitor, arguing against a functional contribution of either PAT1 or CFTR in DRA-mediated Cl/HCO_3 exchange (n = 8–10 for each group).

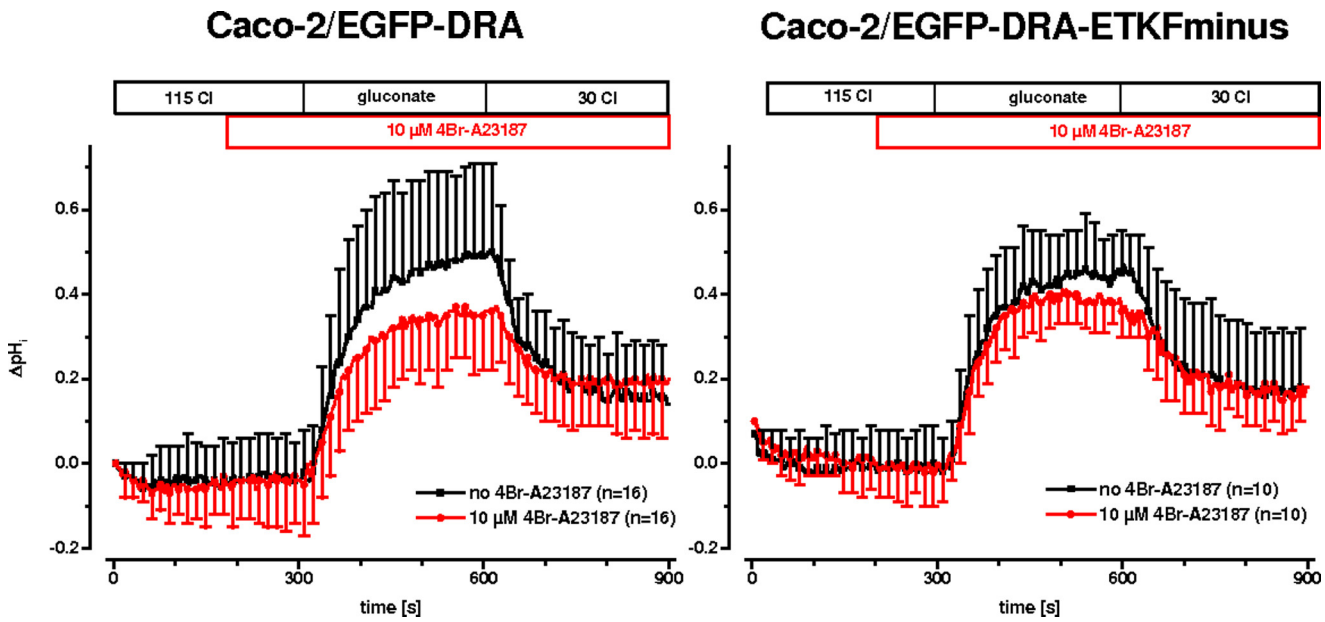

FIGURE 6. **Calcium-mediated inhibition of DRA in Caco-2/BBE cells.** In Caco-2/BBE cells transfected with EGFP-DRA (*left panel*) or transfected with EGFP-DRA-ETKFminus (*right panel*), intracellular calcium was elevated by 4Br-A23187. This leads to an inhibition of DRA activity only in Caco-2/BBE/EGFP-DRA (maximal pH_i change −26%, $p < 0.05$; initial slope −30%, $p > 0.05$, $n = 16$ for each group), suggesting that the PDZ interaction motif was required for calcium-mediated inhibition. Caco-2/BBE/EGFP-DRA-ETKFminus was not inhibited (ΔpH_i 0.54 ± 0.07, −12%, $p > 0.05$; initial slope 0.66 ± 0.40 pH/min *versus* 0.63 ± 0.24, −8%, $p > 0.05$; $n = 10$ for each group).

μM DIDS, a concentration that predominantly inhibits PAT1 but not DRA (27) (maximal ΔpH_i, 0.44 ± 0.12 *versus* 0.45 ± 0.18, 2% stimulation, $p > 0.05$; and initial slope 0.37 ± 0.08 pH/min *versus* 0.37 ± 0.10, 0% change, $p > 0.05$). Furthermore, inhibition of CFTR by 10 μM CFTRinh-172 (28) also had no effect on Cl/HCO_3 exchange activity (maximal ΔpH_i 0.50 ± 0.13 *versus* 0.50 ± 0.11, 0% change, $p > 0.05$; and initial slope 0.42 ± 0.07 pH/min *versus* 0.42 ± 0.13, 0% change, $p > 0.05$) arguing against a functional interplay between CFTR and DRA in these cells. Taken together the data presented in Figs. 3–5 suggest that EGFP-DRA- and EGFP-DRA-ETKFminus-transfected Caco-2/BBE cells are a useful model to study DRA and the potential role of its interaction with PDZ adapter proteins.

Calcium-mediated Inhibition of DRA in Caco-2/BBE Cells—The effect of 4Br-A23187 on Cl/HCO_3 exchange mediated by DRA was then tested in the transfected Caco-2/BBE cells. In wild type EGFP-DRA-transfected cells, 4Br-A23187 inhibited the maximal increase of pH_i after chloride removal significantly by 26% (ΔpH_i, 0.59 ± 0.19 *versus* 0.44 ± 0.11, $p < 0.05$), and the initial slope nonsignificantly by 30% (0.61 ± 0.34 pH/min *versus* 0.42 ± 0.16, $p > 0.05$). In the mutant lacking the PDZ interaction motif (EGFP-DRA-ETKFminus) neither the maximal pH_i increase (ΔpH_i, 0.54 ± 0.07, −12%, $p > 0.05$) nor the initial slope (0.66 ± 0.40 pH/min *versus* 0.63 ± 0.24, −8%, $p > 0.05$) was significantly reduced (Fig. 6). This suggests that calcium-mediated inhibition of DRA involves the interaction of DRA with PDZ adapter proteins in Caco-2/BBE cells and, by extension, in enterocytes.

Because 4Br-A23187 as an ionophore leads to a nonphysiologic elevation of intracellular calcium, the calcium effect needed to be verified by a physiological agonist. Therefore, we tested UTP because it acts via stimulation of P2Y receptors and is independent of protein kinase C (29). Furthermore, postconfluent Caco-2 cells express P2Y receptors that can be stimulated by UTP resulting in an increase of intracellular calcium (30). This effect was confirmed in our EGFP-DRA-expressing cells by comparing the magnitude of the calcium transient induced by 4Br-A23187 with that induced by 100 μM UTP (Fig. 7). As expected the calcium signal was much greater after calcium ionophore than after stimulation with 100 μM UTP. Similar results were found in EGFP-DRA-ETKFminus-expressing cells (data not shown). More importantly, superfusion of 100 μM UTP caused a significant inhibition of the maximal pH_i change (ΔpH_i, 0.66 ± 0.09 *versus* 0.55 ± 0.09, −16%, $p < 0.05$) without affecting the initial slope (0.92 ± 0.35 pH/min *versus*

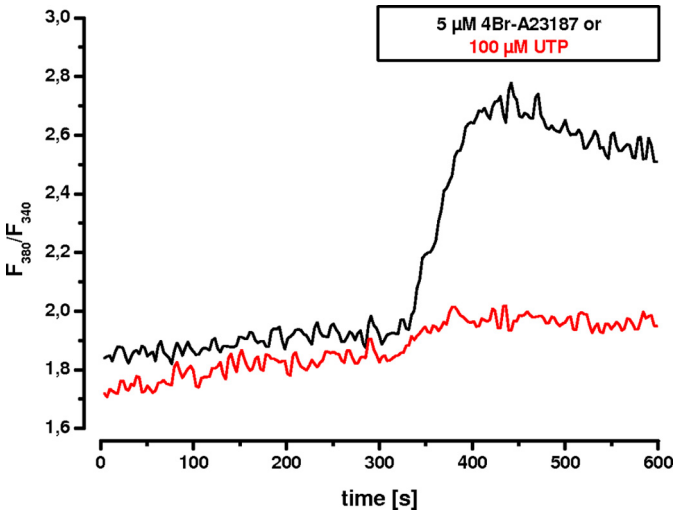

FIGURE 7. **Calcium transients induced by 4Br-A23187 and UTP in transfected Caco-2/BBE cells.** Calcium transients were measured in FURA-2 loaded, EGFP-DRA-expressing Caco-2/BBE cells in response to 5 μM 4Br-A23187 and 100 μM UTP. The magnitude of the calcium signal induced by 4Br-A23187 is much higher than that induced by 100 μM UTP. Representative traces of five experiments each are shown.

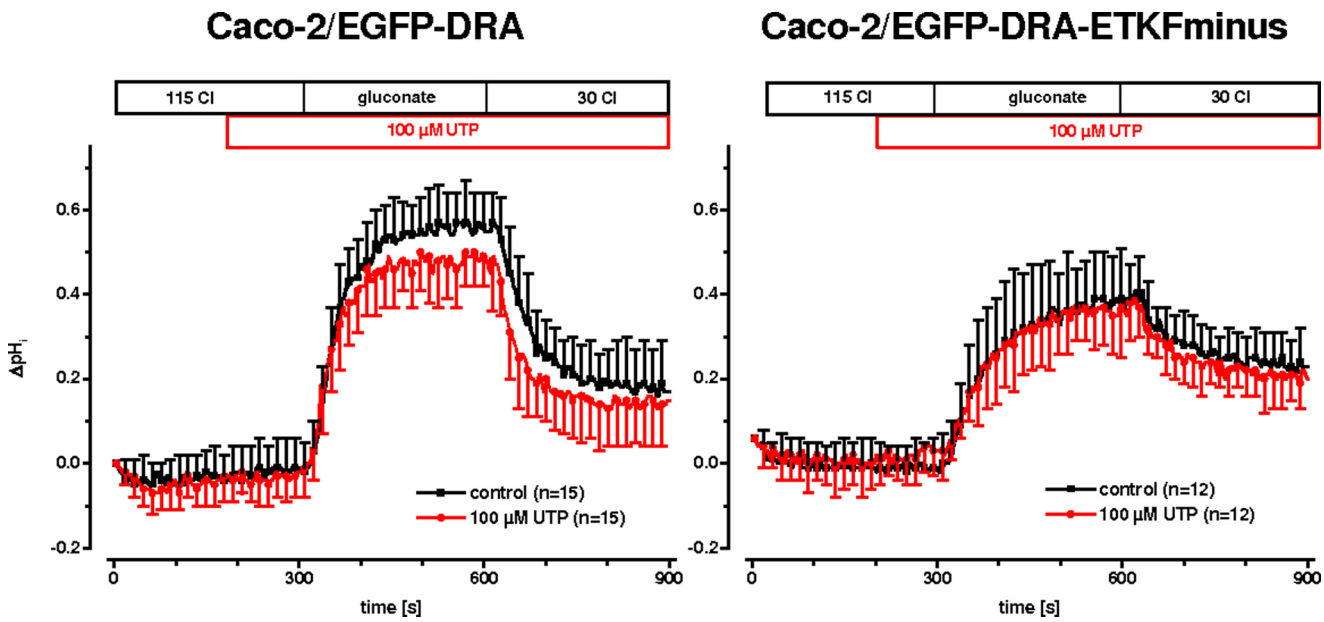

FIGURE 8. **Purinergic receptor stimulation inhibits DRA in Caco-2/BBE cells.** Postconfluent Caco-2 cells possess P2Y receptors that can be stimulated by UTP to induce physiologic intracellular calcium signals. 100 μM UTP inhibited DRA activity only in Caco-2/BBE cells transfected with wild type DRA (*left panel*, maximal pH_i change −16%, $p < 0.05$, initial slope −1%, $p > 0.05$; $n = 15$ for each group) but not in cells transfected with the DRA mutant lacking the PDZ interaction motif (*right panel*, maximal pH_i change −1%, $p > 0.05$, initial slope −1%, $p > 0.05$; $n = 12$ for each group).

0.90 ± 0.38, −1%, $p > 0.05$) only of wild type DRA while leaving the mutated DRA-ETKFminus unaffected (maximal ΔpH_i 0.41 ± 0.12 *versus* 0.40 ± 0.11, −1%, $p > 0.05$; and initial slope 0.40 ± 0.18 pH/min *versus* 0.39 ± 0.15, −1%, $p > 0.05$) (Fig. 8). Again this suggests that the PDZ interaction of DRA plays an important role for the signal transduction of physiologic changes of intracellular calcium on DRA activity.

UTP Inhibition of DRA Is Dependent on PDZK1—HEK cells also express P2Y receptors that are coupled to intracellular calcium (31). Therefore, we repeated the UTP experiment in DRA-transfected HEK cells. Unexpectedly, wild type DRA was not inhibited by UTP in these cells, although the calcium signal was intact (Fig. 9, *A* and *B*).

To resolve the discrepancy of PDZ-dependent inhibition of DRA by UTP in Caco-2/BBE cells and the lack of it in HEK cells, we tested the expression NHERF, E3KARP, PDZK1, and IKEPP in Caco-2, Caco-2/BBE, and HEK cells. We have previously shown that NHERF, E3KARP, and PDZK1 (also known as CAP70) interact with DRA (32, 33), and unpublished data from our laboratory indicate that IKEPP also interacts with DRA.[3] Fig. 9*C* shows that all three cell types express all four PDZ adapter proteins. But the relative expression of E3KARP and PDZK1 in HEK cells is much lower than in Caco-2 and Caco-2/BBE cells.

Because PDZK1 has recently been shown *in vivo* to be required for calcium inhibition of electroneutral NaCl absorption (34), we stably transfected PDZK1 into HEK/EGFP-DRA cells to test whether this would establish UTP inhibition of DRA. PDZK1 was expressed as an N-terminal EGFP fusion construct. We have previously shown that this construct interacts with DRA *in vivo* (33). Fig. 9*D* shows that UTP inhibited DRA in HEK/EGFP-DRA cells that were stably transfected with EGFP-PDZK1 (maximal ΔpH_i, 0.53 ± 0.07 *versus* 0.44 ± 0.07, −18%, $p < 0.05$, initial slope 0.82 ± 0.19 pH/min *versus* 0.61 ± 0.20, −25%, $p < 0.05$). This extends the findings in Caco-2 cells and suggests that PDZK1 plays a prominent role in UTP-induced inhibition of DRA.

Inhibition of DRA by Intracellular Calcium Does Not Occur through Decreased Cell Surface Expression—The activity of transport proteins can be regulated by changes in plasma membrane abundance or by effects on membrane resident transporters. Furthermore, PDZK1 has been implicated in the cell surface expression of various transport proteins (35, 36). To test this, DRA cell surface expression was assayed by biotinylation. In three experiments the amount of EGFP-DRA expressed in the cell surface was not significantly changed after 100 s of treatment with 5 μM 4Br-A23187 (−14 ± 10%, $p > 0.05$; $n = 3$).

DISCUSSION

This study was undertaken to test whether DRA is regulated by elevated intracellular calcium and to determine whether this involves interactions with PDZ adapter proteins. This question was based on the following: (*a*) the known function of DRA in electroneutral NaCl absorption (1, 3); (*b*) the known and well characterized inhibition of NHE3 by intracellular calcium, which involves complex formation with PDZ adapter proteins (19, 22, 37, 38); (*c*) the known interaction of DRA with PDZ adapter proteins of the NHERF class (32, 33); and (*d*) the assumption that DRA should be inhibited in parallel with NHE3. Nevertheless, parallel inhibition of NHE3 and DRA may not necessarily involve individual inhibition of DRA. It was also conceivable that DRA and NHE3 are inhibited together in one structurally coupled complex. Alternatively, DRA could also be inhibited secondarily to NHE3 by its pH_i dependence, which results in a lower activity at more acidic pH_i (18).

[3] G. Lamprecht and D. Natour, unpublished data.

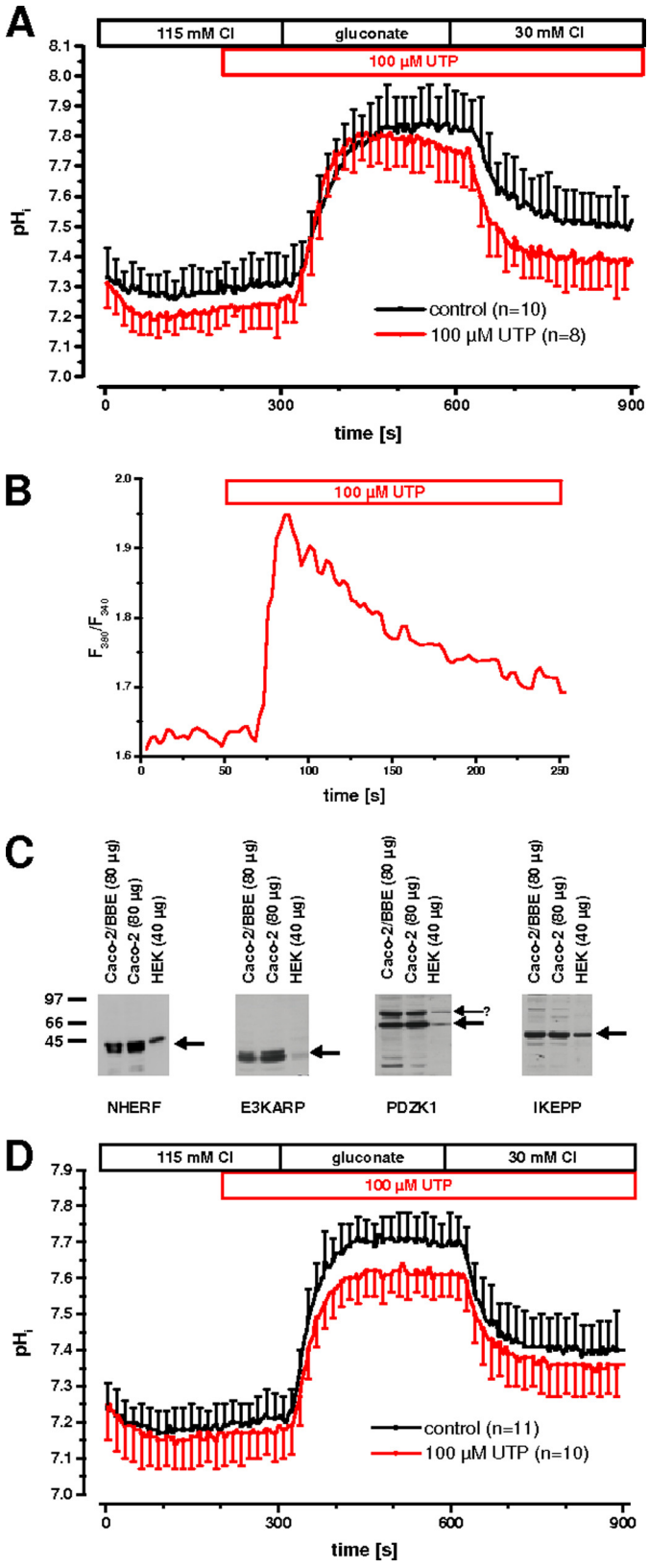

FIGURE 9. **UTP inhibition of DRA is dependent on PDZK1.** *A* and *B*, in HEK cells transfected only with EGFP-DRA, there is no inhibition of Cl/HCO_3 exchange activity by 100 μM UTP ($n = 8-10$ for each group) (*A*) despite a typical peak and plateau-type elevation of intracellular calcium (*B*). *C*, lysates from 14-day confluent Caco-2 and Caco-2/BBE cells and from HEK cells were tested for the expression of endogenous NHERF, E3KARP, PDZK1, and IKEPP. Note that in HEK cells E3KARP and PDZK1 are relatively underexpressed. The nature of the upper band detected by the anti-PDZK1 antibody (*arrowhead*) is unknown. *D*, UTP inhibits DRA activity (maximal pH_i change −18%, $p < 0.05$; initial slope −25%, $p < 0.05$; $n = 10-11$ for each group) in HEK/EGFP-DRA cells that are stably transfected with EGFP-PDZK1.

We have used our previously established model of stably transfected HEK cells (15), which do not express endogenous NHE3 or CFTR, and a newly generated model of stably transfected Caco-2/BBE cells, which express very little NHE3 detected by semiquantitative RT-PCR (Fig. 3) and by functional assay (data not shown). Furthermore, we have studied a DRA mutant that lacks the PDZ interaction motif (DRA-ETKF-minus) to address the role of the PDZ interaction. This approach can only be taken in transfected cells and not in an animal model.

Our nonlinear curve-fitting algorithm of the pH_i traces, which is described in detail in Ref. 18, calculates for each individual tracing the initial slope and the maximal change in pH_i after change from chloride-containing to chloride-free buffers. These values are then used for the statistical analysis. Using this analytical approach, we have previously obtained evidence that DRA is activated by alkaline pH_i (18), a finding that was recently corroborated (39). Regulation of transport activity of DRA may principally occur through changes in V_{max} (by changing the number of DRA molecules in the plasma membrane or by effects on the membrane resident transporter molecules) or by changes of the pH_i dependence of the transporter (the so-called set point). Both in transfected HEK and in transfected Caco-2/BBE cells, elevation of intracellular calcium had its major effect on the maximal change in pH_i, whereas the initial slope was only affected when there were large effects on the maximal change in pH_i. This is indirect evidence that elevation of intracellular calcium affects the pH_i dependence of the transporter, because changes in V_{max} should always be reflected in changes of both the initial slope and the maximal pH_i change. This is also supported by the lack of significant reduction of EGFP-DRA surface expression after 100 s of treatment with 4Br-A23187, a time point at which DRA activity was inhibited 26%. Furthermore, in our model of polarized Caco-2/BBE cells, we are measuring only gradient-driven transport across the apical membrane. This needs to be taken into account when interpreting the magnitude of the effects on the maximal pH_i change. Under physiological conditions of transcellular transport, small changes in the set point of DRA may translate into much larger effects on transcellular absorption of chloride (and sodium, mediated by NHE3).

In our previous work we did not find Cl/HCO_3 exchange mediated by DRA to be electrogenic, *i.e.* with a coupling ratio of 2 Cl for 1 HCO_3, but this is controversial (13, 15, 39–41). If DRA is electrogenic, inhibition by increased intracellular calcium may alternatively occur indirectly through changes in membrane potential, *i.e.* by depolarization of the cell and thus decreased electrochemical driving force.

Recently DRA has been shown to be inhibited together with NHE3 (or NHE2) in double-transfected Caco-2/BBE cells in response to 15 min of treatment with 8-(4-chlorophenylthio)-adenosine 3,5-cyclic monophosphate or thapsigargin (14). This elegant study proved the functional coupling of DRA and NHE3

and demonstrated regulatory effects on transcellular transport of ^{22}Na and ^{36}Cl. These effects were accompanied by reduced cell surface expression of DRA. In our experiments calcium inhibition of DRA after 100 s was not accompanied by reduced cell surface expression. At later time points (when calcium-mediated inhibition of DRA did not progress), the amount of DRA surface expression decreased (data not shown). Thus it appears possible that calcium inhibition of DRA is a two-step process involving early inhibition of transporters in the plasma membrane as well as later retrieval of transporters from the membrane. A similar scenario has been described for dopamine-induced inhibition of NHE3 in the kidney (42).

Using different receptors and signaling pathways, several physiologically important extracellular signals (carbachol, serotonin, *Escherichia coli* heat-stable toxin b, and rotavirus enterotoxin NSP5) eventually lead to an elevation of the intracellular calcium concentration and to inhibition of NaCl absorption (11, 14). In the case of NHE3 inhibition, this involves either the formation of a complex of NHE3, E3KARP, α-actinin-4, and PKC (19, 22, 37) or the dissociation of a complex containing NHE3 and PDZK1 (38).

We have previously shown that PDZK1 also strongly interacts with DRA (33), but at that time we could not characterize the physiological function of the interaction. In this study inhibition of DRA was independent of its PDZ interaction in HEK cells after generation of high intracellular calcium concentrations by the ionophore 4Br-A23187. The physiological calcium signal induced by UTP was intact but required supplementation with exogenous PDZK1 to establish PDZ-dependent inhibition of DRA. These data suggest that PDZK1 targets or tailors physiological and comparably small calcium elevations to the effector protein DRA. In HEK cells, on the other hand, the non-physiologic high calcium levels induced by 4Br-A23187 probably override this targeting of the calcium signal, and thus the inhibition of DRA by 4Br-A23187 appears independent of the PDZ interaction. The molecular mechanism by which PDZK1 mediates calcium-induced inhibition of DRA is currently unknown. It most likely involves additional proteins binding to PDZK1 and maybe also to DRA.

PDZK1 has been shown to mediate NHE3 inhibition in transfected cells (38). Furthermore, colonic surface cells from PDZK1 knock-out mice show loss of calcium inhibition of NHE3 (34). In these colonic surface cells NHE3 and DRA are coexpressed (32). Thus PDZK1 apparently has a prominent role in the calcium-mediated inhibition of NaCl absorption.

In principle, the requirement of PDZK1 for calcium inhibition of DRA shown by the present data could also act at the P2Y receptor or on any other target between the receptor and DRA. Of the various P2Y receptor isoforms P2Y2 and P2Y4 have been characterized in the colon, where they mediate increased chloride secretion by elevation of intracellular calcium (43). Caco-2 cells express P2Y6 receptors in addition to the P2Y2 and P2Y4 isoforms (44), which also signal through intracellular calcium. HEK cells on the other hand express P2Y1, P2Y2, and P2Y4 receptors (31). Of these isoforms only P2Y1 receptors have been shown to specifically interact with E3KARP but not with PDZK1 (45). Furthermore, the C-terminal tails of the other isoforms do not suggest that they include a type I PDZ interaction motif. Taken together, these data suggest that PDZK1 does not act on the level of the P2Y receptor. Furthermore, the P2Y2 or the P2Y4 receptor is most likely the isoform that mediates the UTP effect in our experiments. P2Y2 and P2Y4 receptors stimulate chloride secretion in the colon (43). Based on our data, it is tempting to speculate that purinergic receptor stimulation may inhibit NaCl absorption in parallel.

In summary we have shown that the intestinal Cl/HCO_3 exchanger DRA is individually and specifically inhibited by physiologic elevation of the intracellular calcium level, that this involves its interaction with PDZ adapter proteins, and that it requires the presence of PDZK1. PDZK1 also has a prominent role in the calcium-mediated inhibition of NHE3. Thus interference with PDZK1-mediated signal transduction may be an attractive target for the treatment of some forms of secretory diarrhea.

Acknowledgment—We thank Jan Richter (Institute of Clinical Physiology, Charité, Berlin, Germany) for help with the confocal imaging.

REFERENCES

1. Schweinfest, C. W., Spyropoulos, D. D., Henderson, K. W., Kim, J. H., Chapman, J. M., Barone, S., Worrell, R. T., Wang, Z., and Soleimani, M. (2006) *J. Biol. Chem.* **281,** 37962–37971
2. Schultheis, P. J., Clarke, L. L., Meneton, P., Miller, M. L., Soleimani, M., Gawenis, L. R., Riddle, T. M., Duffy, J. J., Doetschman, T., Wang, T., Giebisch, G., Aronson, P. S., Lorenz, J. N., and Shull, G. E. (1998) *Nat. Genet.* **19,** 282–285
3. Moseley, R. H., Höglund, P., Wu, G. D., Silberg, D. G., Haila, S., de la Chapelle, A., Holmberg, C., and Kere, J. (1999) *Am. J. Physiol.* **276,** G185–G192
4. Walker, N. M., Simpson, J. E., Brazill, J. M., Gill, R. K., Dudeja, P. K., Schweinfest, C. W., and Clarke, L. L. (2009) *Gastroenterology* **136,** 893–901
5. Jacob, P., Rossmann, H., Lamprecht, G., Kretz, A., Neff, C., Lin-Wu, E., Gregor, M., Groneberg, D. A., Kere, J., and Seidler, U. (2002) *Gastroenterology* **122,** 709–724
6. Ko, S. B., Shcheynikov, N., Choi, J. Y., Luo, X., Ishibashi, K., Thomas, P. J., Kim, J. Y., Kim, K. H., Lee, M. G., Naruse, S., and Muallem, S. (2002) *EMBO J.* **21,** 5662–5672
7. Ko, S. B., Zeng, W., Dorwart, M. R., Luo, X., Kim, K. H., Millen, L., Goto, H., Naruse, S., Soyombo, A., Thomas, P. J., and Muallem, S. (2004) *Nat. Cell Biol.* **6,** 343–350
8. Lamprecht, G., and Seidler, U. (2006) *Am. J. Physiol. Gastrointest. Liver Physiol.* **291,** G766–777
9. Donowitz, M., Milgram, S., Murer, H., Kurachi, Y., Yun, C., and Weinman, E. (2005) *J. Physiol.* **567,** 1
10. Field, M. (2003) *J. Clin. Invest.* **111,** 931–943
11. Donowitz, M., and Li, X. (2007) *Physiol. Rev.* **87,** 825–872
12. Clayburgh, D. R., Musch, M. W., Leitges, M., Fu, Y. X., and Turner, J. R. (2006) *J. Clin. Invest.* **116,** 2682–2694
13. Chernova, M. N., Jiang, L., Shmukler, B. E., Schweinfest, C. W., Blanco, P., Freedman, S. D., Stewart, A. K., and Alper, S. L. (2003) *J. Physiol.* **549,** 3–19
14. Musch, M. W., Arvans, D. L., Wu, G. D., and Chang, E. B. (2009) *Am. J. Physiol. Gastrointest. Liver Physiol.* **296,** G202–210
15. Lamprecht, G., Baisch, S., Schoenleber, E., and Gregor, M. (2005) *Pflugers Arch.* **449,** 479–490
16. Shen, L., Black, E. D., Witkowski, E. D., Lencer, W. I., Guerriero, V., Schneeberger, E. E., and Turner, J. R. (2006) *J. Cell Sci.* **119,** 2095–2106
17. Boyarsky, G., Ganz, M. B., Sterzel, R. B., and Boron, W. F. (1988) *Am. J. Physiol.* **255,** C844–856
18. Lamprecht, G., Schaefer, J., Dietz, K., and Gregor, M. (2006) *Pflugers Arch.* **452,** 307–315

19. Kim, J. H., Lee-Kwon, W., Park, J. B., Ryu, S. H., Yun, C. H., and Donowitz, M. (2002) *J. Biol. Chem.* **277,** 23714–23724
20. Yun, C. H., Lamprecht, G., Forster, D. V., and Sidor, A. (1998) *J. Biol. Chem.* **273,** 25856–25863
21. Liedtke, C. M., Yun, C. H., Kyle, N., and Wang, D. (2002) *J. Biol. Chem.* **277,** 22925–22933
22. Lee-Kwon, W., Kim, J. H., Choi, J. W., Kawano, K., Cha, B., Dartt, D. A., Zoukhri, D., and Donowitz, M. (2003) *Am. J. Physiol. Cell Physiol.* **285,** C1527–1536
23. Cohen, M. E., Wesolek, J., McCullen, J., Rys-Sikora, K., Pandol, S., Rood, R. P., Sharp, G. W., and Donowitz, M. (1991) *J. Clin. Invest.* **88,** 855–863
24. Levine, S. A., Nath, S. K., Yun, C. H., Yip, J. W., Montrose, M., Donowitz, M., and Tse, C. M. (1995) *J. Biol. Chem.* **270,** 13716–13725
25. Janecki, A. J., Montrose, M. H., Zimniak, P., Zweibaum, A., Tse, C. M., Khurana, S., and Donowitz, M. (1998) *J. Biol. Chem.* **273,** 8790–8798
26. Chapman, J. M., Knoepp, S. M., Byeon, M. K., Henderson, K. W., and Schweinfest, C. W. (2002) *Cancer Res.* **62,** 5083–5088
27. Mount, D. B., and Romero, M. F. (2004) *Pflugers Arch.* **447,** 710–721
28. Ma, T., Thiagarajah, J. R., Yang, H., Sonawane, N. D., Folli, C., Galietta, L. J., and Verkman, A. S. (2002) *J. Clin. Invest.* **110,** 1651–1658
29. Bucheimer, R. E., and Linden, J. (2004) *J. Physiol.* **555,** 311–321
30. Inoue, C. N., Woo, J. S., Schwiebert, E. M., Morita, T., Hanaoka, K., Guggino, S. E., and Guggino, W. B. (1997) *Am. J. Physiol.* **272,** C1862–1870
31. Fischer, W., Franke, H., Gröger-Arndt, H., and Illes, P. (2005) *Naunyn Schmiedebergs Arch. Pharmacol.* **371,** 466–472
32. Lamprecht, G., Heil, A., Baisch, S., Lin-Wu, E., Yun, C. C., Kalbacher, H., Gregor, M., and Seidler, U. (2002) *Biochemistry* **41,** 12336–12342
33. Rossmann, H., Jacob, P., Baisch, S., Hassoun, R., Meier, J., Natour, D., Yahya, K., Yun, C., Biber, J., Lackner, K. J., Fiehn, W., Gregor, M., Seidler, U., and Lamprecht, G. (2005) *Biochemistry* **44,** 4477–4487
34. Cinar, A., Chen, M., Riederer, B., Bachmann, O., Wiemann, M., Manns, M., Kocher, O., and Seidler, U. (2007) *J. Physiol.* **581,** 1235–1246
35. Anzai, N., Miyazaki, H., Noshiro, R., Khamdang, S., Chairoungdua, A., Shin, H. J., Enomoto, A., Sakamoto, S., Hirata, T., Tomita, K., Kanai, Y., and Endou, H. (2004) *J. Biol. Chem.* **279,** 45942–45950
36. Thomson, R. B., Wang, T., Thomson, B. R., Tarrats, L., Girardi, A., Mentone, S., Soleimani, M., Kocher, O., and Aronson, P. S. (2005) *Proc. Natl. Acad. Sci. U.S.A.* **102,** 13331–13336
37. Li, X., Zhang, H., Cheong, A., Leu, S., Chen, Y., Elowsky, C. G., and Donowitz, M. (2004) *J. Physiol.* **556,** 791–804
38. Zachos, N. C., Li, Y., Kovbasnjuk, O., Sarkar, R., Hogema, B. M., de Jonge, H., and Donowitz, M. (2006) *Gastroenterology* **130** (Abstr. 51)
39. Hayashi, H., Suruga, K., and Yamashita, Y. (2009) *Am. J. Physiol. Cell Physiol.* **296,** C1279–1290
40. Melvin, J. E., Park, K., Richardson, L., Schultheis, P. J., and Shull, G. E. (1999) *J. Biol. Chem.* **274,** 22855–22861
41. Shcheynikov, N., Wang, Y., Park, M., Ko, S. B., Dorwart, M., Naruse, S., Thomas, P. J., and Muallem, S. (2006) *J. Gen. Physiol.* **127,** 511–524
42. Hu, M. C., Fan, L., Crowder, L. A., Karim-Jimenez, Z., Murer, H., and Moe, O. W. (2001) *J. Biol. Chem.* **276,** 26906–26915
43. Leipziger, J. (2003) *Am. J. Physiol. Renal Physiol.* **284,** F419–432
44. McAlroy, H. L., Ahmed, S., Day, S. M., Baines, D. L., Wong, H. Y., Yip, C. Y., Ko, W. H., Wilson, S. M., and Collett, A. (2000) *Br. J. Pharmacol.* **131,** 1651–1658
45. Fam, S. R., Paquet, M., Castleberry, A. M., Oller, H., Lee, C. J., Traynelis, S. F., Smith, Y., Yun, C. C., and Hall, R. A. (2005) *Proc. Natl. Acad. Sci. U.S.A.* **102,** 8042–8047